

FIELD STUDY ON THE NEARSHORE SEDIMENT PROCESS AROUND THE TENRYU ESTUARY USING IMAGE ANALYSIS

Haijiang Liu¹, Yoshimitsu Tajima¹ and Shinji Sato¹

A field investigation, based on the shore-based video technique, was conducted to estimate the temporal and spatial variation of the nearshore sediment process at Tenryu estuary, Japan. Image analysis with a new boundary detection technique and an improved rectification approach was used on the recorded images. A case study, by focusing on the time period from Jul to Sep, 2007 when significant typhoon and flood visited the relevant region, was carried out to reveal the qualitative and quantitative insights into the corresponding morphodynamic behaviors.

INTRODUCTION

The nearshore zone is of significant social importance for human beings. Investigation on the present state of beaches and coastlines, together with predicting future situations in terms of a variety of timescales, is critical for understanding the physical mechanism and providing the suitable management of our precious coastal resources.

At the same time, such field research activities are embarrassed by the hostile field weather conditions. In-situ survey methods provide excellent data but require significant man power, major logistical commitments and often lack spatiotemporal resolution to resolve processes of interest. In the last two decades, being an indirect measurement, shore-based video monitoring techniques are applied to interpret the remotely sensed information in terms of relevant hydrodynamic and morphological parameters. Among those, the advanced ARGUS system developed at Oregon State University (Lippmann and Holman, 1989) enables the monitoring of various nearshore features at spatiotemporal scales of direct management and research interests (meters-kilometers and hours-days). Recently, the ARGUS station was used as a basic tool for the CoastView Program. Through it, comprehensive studies have been conducted to bridge the communications gap between research outcomes and products of value to managers. A series of CoastView methodologies, called video-derived Coastal State Indicators (CSIs), has been developed and delivered in a timely manner to managers with a ground truth. The “frame of reference” approach developed by CoastView has been fully summarized and reviewed through a special issue in *Coastal Engineering* (2007, 54(6-7), 461-576).

Up to now, in total, 26 ARGUS stations were constructed around the world (Aarninkhof, 2003). However, only a few of them pay attention to the estuary

¹ Department of Civil Engineering, The University of Tokyo, 7-3-1 Hongo, Bunkyo-ku, Tokyo, 113-8656, Japan

area where the spatiotemporal variation of the morphodynamic behavior is rather significant. The ARGUS station established at Teignmouth, UK is overlooking a dynamic estuarine inlet with an ebb tidal delta sandbar system. The relative inlet morphodynamics has been studied by Siegle et al. (2007) through coupling video imaging and numerical modeling. In Japan, a series of Typhoons, together with the corresponding river floods, attacks the coastal region frequently. Such energetic period complicates the situation for our understanding and management. At the same time, during these extreme events, dramatic local morphology change may occur in an instant mode at a certain place that we can not predict beforehand. Comprehensive investigation is needed to reinforce our knowledge on the estuary morphodynamics.

In this study, by applying the shore-based video technique, a field investigation was conducted to focus on the dynamic behavior at the Tenryu estuary, Japan. Attentions concentrate over a period from Jul to Sep, 2007, when two extreme Typhoons visited this region. Three field cameras were used to acquire the real-time images. Image analysis was used for data processing. Two methodologies were considered here, boundary detection and image rectification. Results are illuminated with respect to the temporal variation and spatial deformation of the river mouth sand spit area. Discussions are specified from both the qualitative and quantitative viewpoints.

STUDY AREA AND RESEARCH APPROACH

In this study, the target area is the Tenryu estuary, which is the conjoint region of Tenryu River and Enshunada Coast and located at the west of Shizuoka Prefecture, Japan (Figure 1). Along the west side of river mouth, a sand spit exists. This region has been suffered from coastal erosion induced by various natural and anthropogenic reasons. Detailed descriptions can be found in Liu et al. (2007). The sand spit morphology and the relevant nearshore bathymetry are rather dynamic with respect to the co-actions from river discharge, daily wave climate and tidal currents. Simultaneously, intermittent extreme events, *e.g.*, typhoons and floods, can cause significant deformation on the topography in an instant mode. This further embarrasses our understanding on the physical phenomena. A qualitative and quantitative insight into the morphodynamic behavior of this area is required.

Taking into account that shore-based video technique, as a cost-efficient method, has the availability to quantify nearshore bathymetry with high resolution in time and space, similar to ARGUS system, field cameras were installed at the both sides of the Tenryu River mouth (Figure 1). On the west side, one camera was fixed on the top of a vent tower at Seien (thereafter refer to as C1) to look at the sand spit region; on the east side, two cameras were set up on the top of a lighthouse at Kaketsuka (thereafter refer to as C2 and C3, respectively) to monitor the sand spit and estuary entrance. The field camera system mainly composes of three components: camera (for data recording), Terastation (for data storage) and UPS (for power protection). Image recording

starts from 5 am to 7 pm everyday. Truecolor images were recorded with JPEG compression for storage. The image has a 1280×960 pixel resolution.

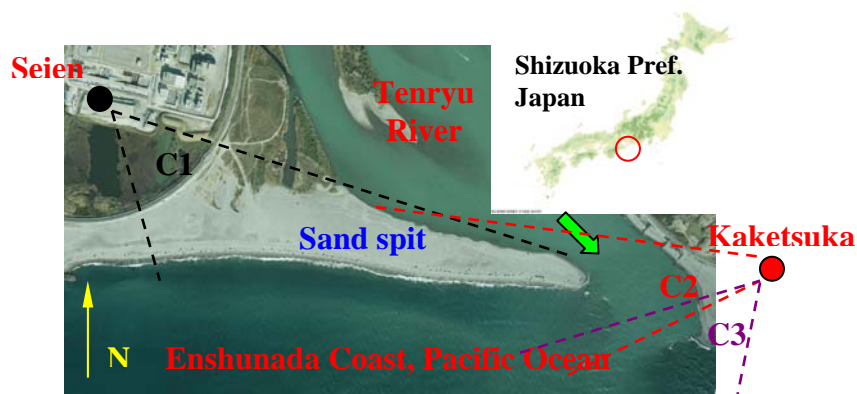


Figure 1. Tenryu Estuary and camera locations, together with their schematic recording azimuths (broken lines).

Different from ARGUS system, which is based on hourly image collection with three different types, *i.e.*, a single snapshot, a 10-min time-exposure and a 10-min variance image (Holman and Stanley, 2007), we recorded images with a time interval of 1.2 s or 10 s. Such a short time interval is considered here because change during typhoon or flood can be in a rather fast pattern, even shorter than one-hour scale. From the recorded images, it is found that the collapse of river mouth sand spit on Jul 15, 2007 was in a quick mode (time scale of minute). Complex deformation process on the relevant morphology can only be observed from the continuously recorded images. Detailed recording can facilitate us to clarify insight into the physical mechanism and has a great value to the subsequent investigation. However, such process may be escaped from the hourly based ARGUS image. In ARGUS system, pixel time series by sampling intensity variations at 2 Hz at one or several representative locations were applied to study nearshore features, *e.g.*, wave period, wave angle, phase speed, wave runup and longshore current (Holman and Stanley, 2007). Nevertheless, it is very difficult for us to define the characteristic points during extreme event since the most dynamic area, such as the sand spit collapsing spot, is somewhat unpredicted both in time and space resolutions. Considering these, the whole image recording was conducted in this study.

IMAGE ANALYSIS

In this section, approaches used for image analysis are specified, which include two sub-topics, *i.e.*, boundary detection to extract the sand spit profile and image rectification/merging to obtain the clear and whole sand spit region. Details are described in the following subsections. To do inter-comparison for the sand spit profile on different days, recorded images at the same tidal level

($T.P.$ equals to zero, in which $T.P.$ stands for the average water level of Tokyo Bay, a standard datum level in Japan) were considered here. Time exposure images (10-min averaged image) were used to outline the natural estuary modulations and remove any moving objects' influence.

Boundary Detection

Figure 2 presents a typical time exposure image recorded from Camera C1 at Seien. The whole sand spit area can be observed in this figure although the camera-far field is blurry. Boundary detection is trying to find this sand spit profile to analyze the spatiotemporal morphodynamic behavior of this region. Considering the shoreline detection in ARGUS system, there are four typical shoreline mapping methods, *i.e.*, the "Shore Line Intensity Maximum" model (SLIM model), the "Color Channel Divergence" model (CCD model), the "Artificial Neural Net" model (ANN model) and the "Pixel Intensity Clustering" model (PIC model). These methods are based on various mechanisms to delineate a shoreline. Detailed descriptions and performance of these models are summarized in Plant et al. (2007). In this study, the sand spit is enclosed by two different circumstances, the south side facing wave-dominant ocean and the north side facing current-dominant river. Here, to determine the sand spit profile, various techniques were introduced. Figure 3 shows the flow chart for boundary detection procedure. Through this procedure, the original truecolor image is converted into a binary image (black and white, two-color image), which is much easier to deal with in terms of further digital image processing, *e.g.*, boundary detection.



Figure 2. A typical time exposure image recorded from Camera C1 at Seien at 9:19 am Jul 2, 2007. Solid line box presents the region of interest.

An RGB image composes of three color matrixes, where each color pixel is a triplet corresponding to the red, green and blue components. It can be viewed as a 'stack' of three gray-scale images. Considering that most of the digital

image processing is for grayscale images. In this study, we first convert the truecolor image into grayscale image as shown in Figure 4(a). Figure 4(b) illustrates the grayscale image intensity histogram. There are several intensity peaks along the gray scale, which correspond to different features in the image. The lowest intensity peak comes from trees since they are dark color in Figure 4(a), and the highest three peaks are ascribed to the sky considering that it is bright. However, for our interests, we are trying to separate sand spit area from water region. As shown in Figure 4(b), these two features are related to the small middle peaks with relatively indistinct intensity values. To extract such blurred components in one image, pre-processing is needed. First of all, region of interest (ROI) was selected as shown in Figure 2 using a solid line box. Considering only this area facilitates our further procedure because much more important information, but much less image region, is included in this part. Another typical feature of the recorded image is non-uniform background intensity. As we can see from Figure 4(a), middle part of the image is somewhat bright; whereas, two sides of the image are dark. To remove such image background inhomogeneity, intensity in the sky region is considered since brightness in this area is more uniform than other regions. With a view to the large intensity value in sky region, the negative image was taken into account as illustrated in Figure 4(c). A representative line, *i.e.*, solid line in Figure 4(c), was selected to delineate the background intensity information. Figure 4(d) demonstrates the cross-image background intensity distribution. Intensity inhomogeneity can be easily found in this image with middle part being small. To mathematically represent this characteristic, cubic curve fitting was applied as shown by the equation in Figure 4(d).

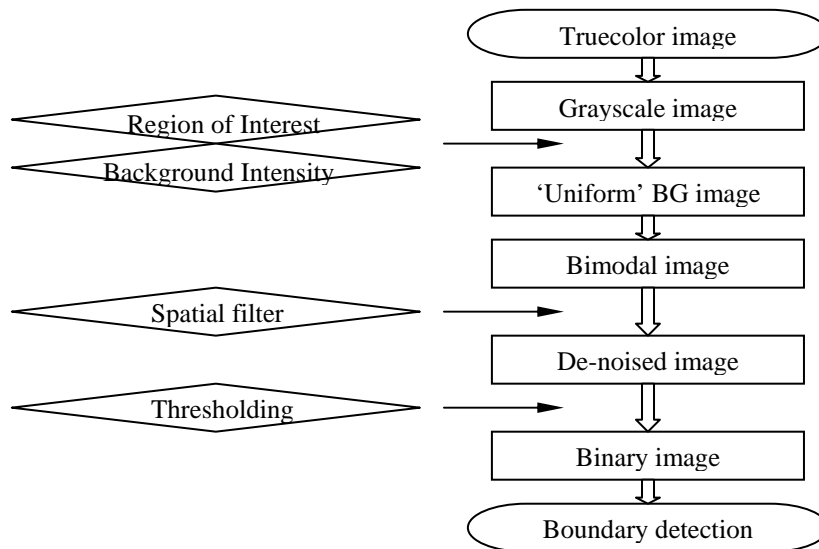


Figure 3. Flow chart for boundary detection procedure in image analysis.

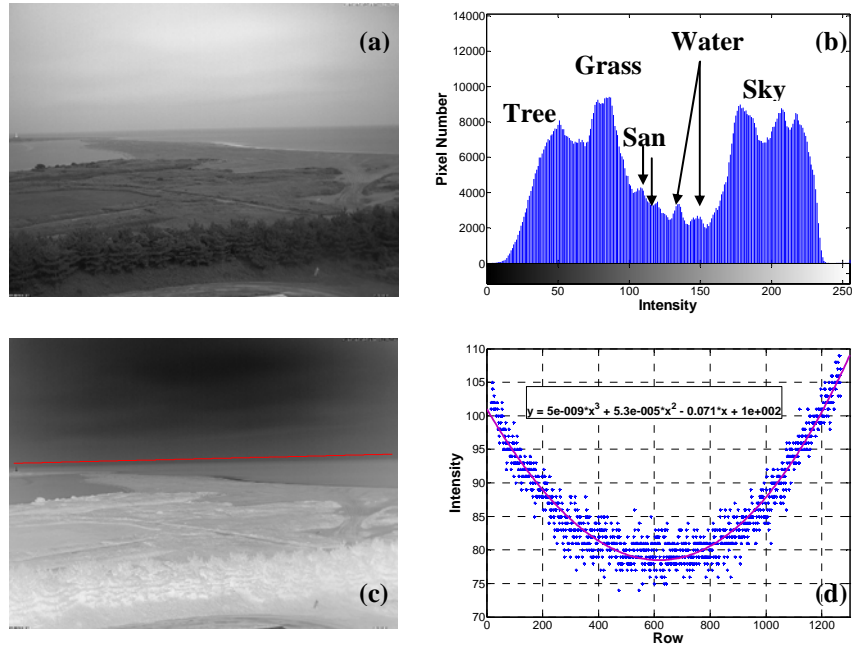


Figure 4. Image processing for an example image in Figure 2. (a) Grayscale image (b) Corresponding intensity histogram. (c) Negative image. Solid line presents a representative line to remove the non-uniform background (d) Background intensity distribution along the representative line.

Applying the curve fitting equation in the region of interest, a ‘uniform’ background (BG) image can be obtained as illustrated in Figure 5(a). This brings a relatively BG-homogeneous image for the subsequent processing. In this image, considering the land area, there still exist significant intensity differences between grass and bald land parts, which cause difficulties with respect to defining a suitable threshold value for the final binary image. Such image still includes several intensity histogram peaks. Taking into account the bald land intensity information, we further modified the ‘uniform’ BG image into a bimodal image, whose intensity histogram only includes two main peaks, *i.e.*, one related to land area and the other related to water area. To further remove the local inhomogeneity, a small disk-type spatial filter was used to the obtained bimodal image. Figure 5(b) shows the filtered bimodal image. In this image, there exists clear intensity difference between water and land area. Simultaneously, intensity distribution is rather uniform within either land or water region, which facilitates searching on the threshold value for binary image. In the next step, either Otsu (1979) method or Gonzalez and Woods (2008) method was introduced to select the global threshold value in applications of image segmentation. Finally, the binary image was obtained as

shown in Figure 5(c). Further binary image processing by applying the approach proposed by Gonzalez and Woods (2008) presents the detected land boundary as shown using a solid line in Figure 5(d) together with the original truecolor image. In general, satisfactory results can be obtained both for the seaside and riverside of the sand spit, especially in the camera-near field. In the camera-far field, however, there exist some boundary detection errors. This is owing to the less pixel information in the recorded image. Such problem will be solved using the merged panoramic rectified image after considering the recorded images on both sides of the estuary, as specified in the following subsection.

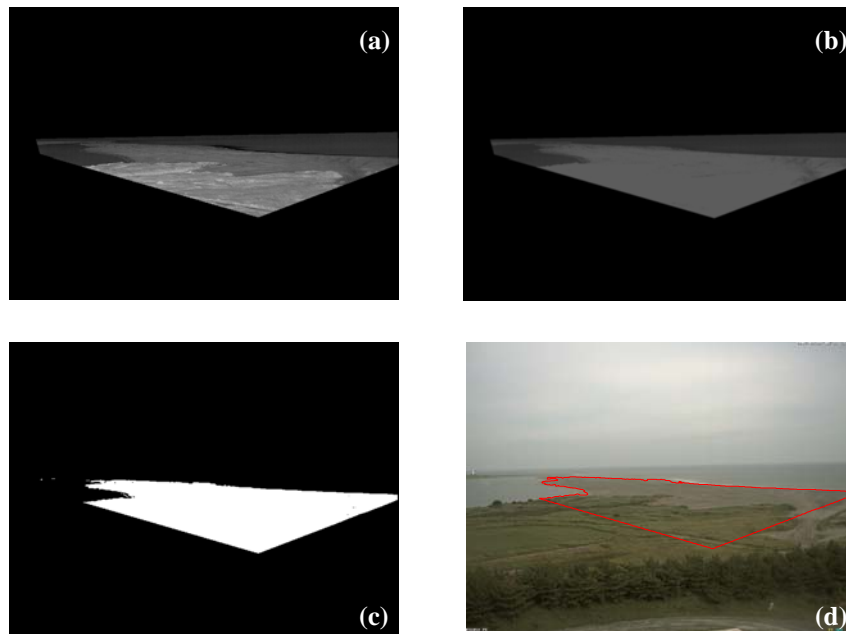


Figure 5. Image processing for an example image in Figure 2. (a) ‘Uniform’ BG image within ROI. (b) De-noised bimodal image within ROI. (c) Binary image. (d) Detected boundary (solid line) in the original image.

Image Rectification/Merging

Quantification of image features requires accurate geo-referencing of oblique video data and a good understanding of the cross-camera variation of pixel resolutions. These aspects are described through the relationship between image coordinate and the corresponding real world location. Holland et al. (1997) have established such relationship for application with the ARGUS system. In this study, similar approach was applied for image rectification to get the plan-view image of the whole sand spit area. However, considering that our

cameras are installed at a relatively low elevation, but far from the target site due to field limitations, weight factors were introduced to improve the rectified image quality by enhancing the role of camera-far-field ground control points (GCP). It is known that moving of one pixel in a recorded image represents different real-world distance, that is, it may only be equal to a few meters in the camera-near field; whereas, such one-pixel shift can induce tens of hundreds meters difference in the camera-far field. This means image pixel plays a different role with respect to the camera calibration with camera far-field GCPs being more important. Taking these into account, the following horizontal and vertical weight functions, w_u and w_v , were introduced,

$$w_u = \frac{1}{\sqrt{\left(\frac{\partial u}{\partial x}\right)^2 + \left(\frac{\partial u}{\partial y}\right)^2}} \quad (1)$$

$$w_v = \frac{1}{\sqrt{\left(\frac{\partial v}{\partial x}\right)^2 + \left(\frac{\partial v}{\partial y}\right)^2}} \quad (2)$$

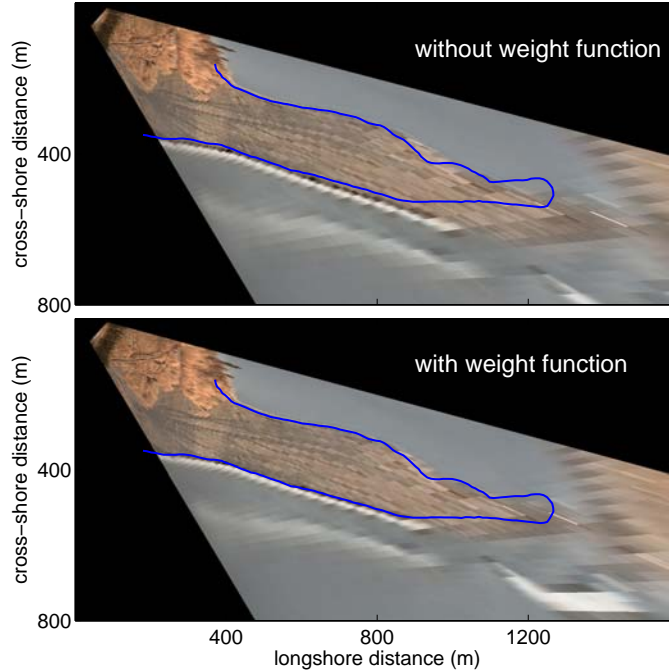


Figure 6. Comparison between the rectified image (C1) without and with weight function. Solid lines represent the synchronously recorded shoreline using GPS.

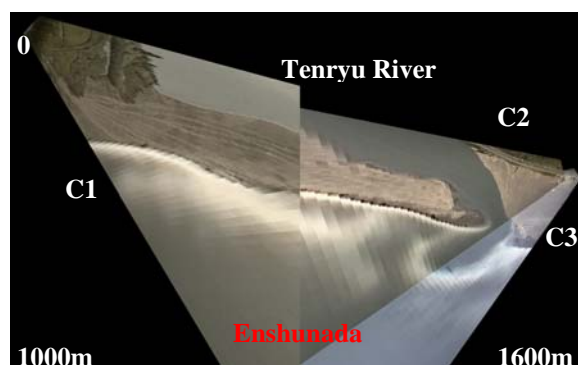


Figure 7. Merged, plan-view time exposure image of Tenryu Estuary from all three cameras. Images were recorded at 8 am, Jul 5, 2007.

where u, v are image coordinates, and x, y are the real-world coordinates. Figure 6 presents a comparison between the rectified image (camera C1) with and without weight function. Improvement can be easily observed after considering the synchronously recorded shoreline position using GPS.

However, due to less pixel information in the camera-far field, rectified image does not show a clear feature even after introduction of weight function. At the same time, as pointed out in the last subsection, boundary detection could not perform well in the camera-far field from the single camera-recorded images. Merged, plan-view image after three cameras (C1, C2 and C3) was introduced as presented in Figure 7. The whole sand spit area and river mouth entrance, as well as the nearby ocean surface, were monitored with an adequate resolution. Several interesting characteristics were revealed from Figure 7. A smooth white band, being an excellent proxy for the underlying, submerged sand bar topography (Lippmann and Holman, 1989), can be clearly distinguished in image. Wave blocking phenomena, due to the convergence of river current and ocean wave, can be observed just in front of the river entrance through a nearly closed white circle. In the following discussions, such merged, plan-view image will be applied.

RESULTS AND DISCUSSIONS

Applying the above-mentioned image analysis approaches, a case study was carried out to investigate the topography modification at Tenryu estuary from Jul to Sep, 2007. During this period, a severe typhoon, No 4, with a significant wave height over 7 m, attacked the research area on Jul 15. Accompanying with it, a serious river flooding occurred. The river mouth sand spit partially collapsed owing to these extreme events. Afterwards, sand spit was gradually recovered. During the recovery process, another typhoon, No 9, with a significant wave height around 6 m, visited this region on Sep 6. All morphodynamic processes were fully recorded by field cameras, which present the firsthand information for study on the whole physical procedure. In this

section, by focusing on the sand spit area, discussion on the processed images is carried out from both the qualitative and quantitative viewpoints.

Qualitative Discussions

Figure 8 presents qualitative results on the sand spit profile in the period of pre-, during- and post-Typhoon. Figure 8(a) shows an example of the merged, plan-view binary image recorded on Jul 16, just after typhoon attacking. In the image, white area demonstrates the of-the-day sand spit profile in the region of interest specified in Figure 2. Whilst, all other regions are described as black color. Applying the boundary detection technique mentioned previously, sand spit profile was extracted for qualitative analysis.

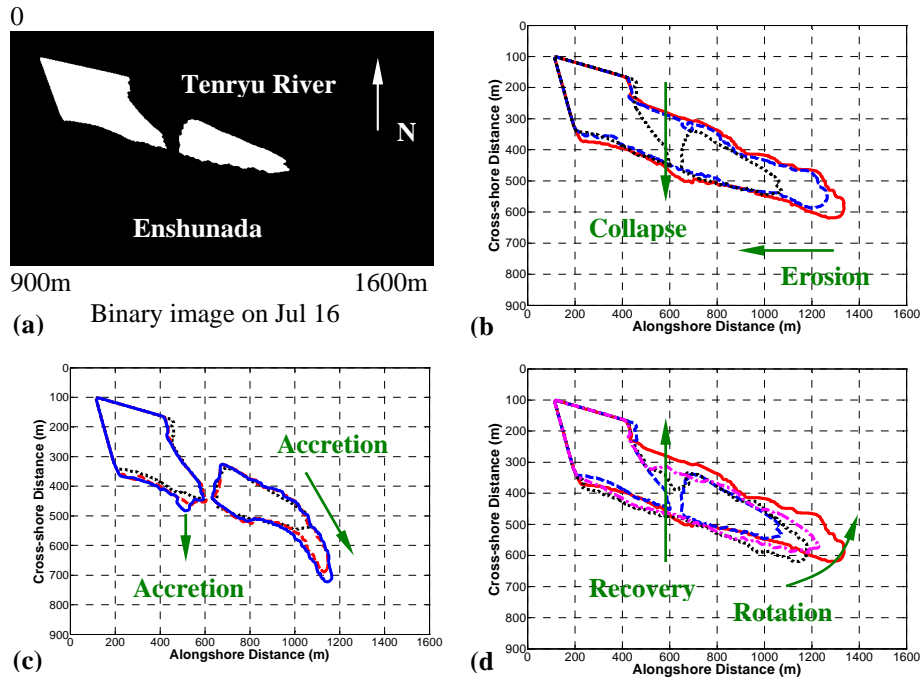


Figure 8. Qualitative discussion on the sand spit profile. (a) Merged, plan-view binary image for sand spit on Jul 16. (b) Sand spit profiles on Jul 2 (solid line), 14 (dashed line) and 16 (dotted line). (c) Sand spit profiles on Jul 16 (dotted line), 20 (dashed line) and 27 (solid line). (d) Sand spit profiles on Jul 2 (solid line), 16 (dashed line), Sep 2 (dotted line) and 8 (dash-dotted line).

Figure 8(b) illustrates the original sand spit profile (Jul 2), just before and after typhoon, No 4 (Jul 14 and 16, respectively). Looking at results on Jul 2 and 14, erosion process occurred at the tip of sand spit, which made river entrance wide to allow the increasing river discharge. Just after typhoon on Jul 16, significant erosion was observed at the tip region. At the same time, the

middle part of sand spit collapsed, which separated the original sand spit into two parts, a remaining sand spit in the west and an isolated island in the east. These two processes, *i.e.*, tip erosion and middle collapse, occurred simultaneously to meet the significant river discharge from upstream flood (a maximum river discharge about $8.7 \times 10^3 \text{ m}^3/\text{s}$). It is found the strong river flow played an important role on the sand spit failure, which moved the relevant sediments to the Enshunada Coast in an instant mode. On the other hand, the recovery process was dominated by the daily wave climate. Figure 8(c) presents the recovering process in July. It is found that deposition took place first at the tip of the isolated island. Sediment accumulation was in the south-east direction, instead of east direction of the original profile. This is ascribed to the strong flows following river flooding. Comparing profiles on Jul 20 and 27, generation in the tip region is rather gradual. Nevertheless, offshore directional accretion also occurred along the seaward of the remaining sand spit area. The reason behind such recovery process was revealed through the measured bathymetry data in Aug, 2007. After Typhoon 4, a large amount of sediments was deposited in front of the cut and tip subaqueous areas. These sands were gradually, but firstly, sent back through the daily wave actions, and emerged in the corresponding region. Figure 8(d) includes another two sand spit profiles on Sep 2 and 8. On Sep 2, the seaside of collapse region was closed and the sand spit was re-connected as a whole unit. At the same time, a remaining riverside cut on the north part still existed where it can not be affected by the normal daily waves. On Sep 6, typhoon 9 visited the target area. Overtopping occurred owing to the extreme wave height. Looking at sand spit profile on Sep 8, it is clear that the riverside cut was fully refilled after typhoon 9 due to the deposited sediments carried by the overtopping waves. As for typhoon 9, the corresponding river discharge ($7.9 \times 10^2 \text{ m}^3/\text{s}$) is much smaller than that of typhoon 4. Therefore, the enlarged river entrance (after typhoon 4) can discharge such amount of upstream flux. Sand spit did not collapse again to increase the outflow since there is no significant water head difference between the riverside and the seaside. Maximum head difference was 0.53 m for typhoon 9, whereas it was much larger for typhoon 4 with a value of 2.77 m. Another interesting phenomenon is the rotation of sand spit head after typhoon 9. Certain part of seaside sediments at the sand spit head was carried to the riverside due to high waves after comparing profiles recorded on Sep 2 and 8.

Quantitative Discussions

Figure 9 presents quantitative analysis on the temporal variation of the sand spit area from Jul to Sep, 2007. The area was estimated through the white part in the merged, plan-view images (Figure 8a). In Figure 9, data shortage was caused by the recorded image ambiguity or some technical problems related to the camera system. It is observed that the whole sand spit covered an area around $2 \times 10^5 \text{ m}^2$ before typhoon 4. During typhoon, almost the whole area was submerged with an emerged area only about $1 \times 10^4 \text{ m}^2$ on Sep 15. This is ascribed to the high river water level owing to the significant river discharge,

not the real sand spit erosion. In general, the river entrance water level is equal to tide level. However, water level at the river entrance was T.P. 2.4 m on Sep 15 when tide level was T.P. 0 m then. After typhoon 4, the whole sand spit area was about $1.5 \times 10^5 \text{ m}^2$. Total loss of the sand spit area between pre- and post-typhoon 4 was about $5 \times 10^4 \text{ m}^2$. From the qualitative analysis, it is clear that the decrease on sand spit area comes from two regions, the tip erosion/retreatment and the middle part collapse. After typhoon 4, the recovery process can be distinguished into two stages. Within July, recovery is in a fast phase as shown using a dashed line in Figure 9. Afterwards, recovery is in a slow/stable phase illustrated by a solid line. Sudden lose on Sep 6 was ascribed to the overtopping effect from typhoon 9. The newly refilled parts, since they were relatively low, were temporally covered by water owing to the significant wave setup (about 1.5 m) from the large wave height (near 6 m).

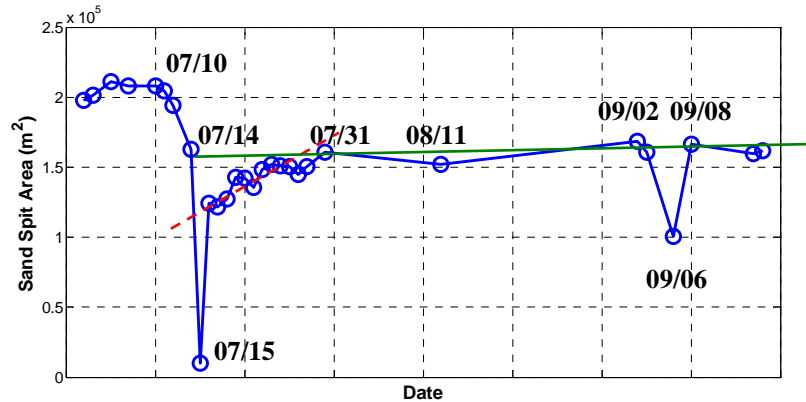


Figure 9. Quantitative analysis on the temporal variation of the sand spit area from Jul to Sep, 2007.

CONCLUSIONS

A field investigation, based on the shore-based video technique, was conducted to estimate the temporal and spatial variation of the nearshore sediment process at Tenryu estuary, Japan. A case study, by focusing on the time period from Jul to Sep, 2007 when significant typhoon and flood passed through the relevant region, was carried out to reveal the qualitative and quantitative insights into the corresponding morphodynamic behaviors. Main conclusions were summarized as follows,

1. A boundary detection technique was established by converting the truecolor image into binary image. It can figure out both the shoreline position and riverside water-land interface.
2. By introducing a weight function to enhance the roles of camera-far field ground control points, image rectification technique was improved.

3. Qualitative analysis on the sand spit profile demonstrates that during typhoon 4, sand spit collapse occurred in an instant mode, and was induced by the strong river flow; whereas, the subsequent recovery process was ascribed to the daily wave climate in a gradual mode.
4. Seaside to riverside recovery can be observed after typhoon No 4. This process starts from the cut and tip regions first. During the recovery, wave overtopping can help to refill the riverside erosion.
5. Quantitative discussion on the sand spit area shows that total loss of sand spit area before and after typhoon 4 was about 5×10^4 m². The recovery went through a two-stage process, a fast phase in July and a slow/stable phase afterwards.

ACKNOWLEDGMENTS

We want to thank Dr. T. Takagawa, the University of Tokyo, for helps during field survey. This study is a part of Tenryu-Enshunada Project financially supported by the Japan Science and Technology Agency (JST).

REFERENCES

- Aarninkhof, S.G.J., 2003. *Nearshore bathymetry derived from video imagery*. PhD thesis, Delft Hydraulics Select Series 3/2003. Delft University of Technology, Delft University Press, Delft, 175 pp.
- González, R.C., and R.E., Woods, 2008. *Digital image processing*. 3rd ed., Prentice Hall, Upper Saddle River, NJ, 954 pp.
- Holland, K.T., R.A., Holman, T.C., Lippmann, and J. Stanley, 1997. Practical use of video imagery in nearshore oceanographic field studies. *IEEE J. of Oceanic Eng.*, 22(1), 81-92.
- Holman, R.A., and J., Stanley, 2007. The history and technical capabilities of Argus. *Coastal Engineering*, 54(6-7), 477-491.
- Lippmann, T.C., and R.A., Holman, 1989. Quantification of sand bar morphology: A video technique based on wave dissipation. *J. of Geophysical Research*, 94(C1), 995-1011.
- Liu, H., S., Sato, Y., Tajima, G., Huang, and H., Fujiwara, 2007. Investigation on the historical evolution of alluvial deposits along the Tenryu River and the Enshu Coast. *Proceedings of the 4th Asian and Pacific Coastal Engineering Conference*, Nanjing, China, 1139-1150.
- Otsu, N., 1979. A threshold selection method from gray-level histograms. *IEEE Trans. Systems, Man, and Cybernetics*, Vol. SMC-9(1), 62-66.
- Plant, N.G., S.G.J., Aarninkhof, I.L., Turner, and K.S., Kingston, 2007. The performance of shoreline detection models applied to video imagery. *J. of Coastal Research*, 23(3), 658-670.
- Siegle, E., D.A., Huntley, and M.A., Davidson, 2007. Coupling video imaging and numerical modeling for the study of inlet morphodynamics. *Marine Geology*, 236, 143-163.

KEYWORDS – ICCE 2008

PAPER TITLE: FIELD STUDY ON THE NEARSHORE SEDIMENT
PROCESS AROUND THE TENRYU ESTUARY USING IMAGE ANALYSIS

Authors: Haijiang LIU, Yoshimitsu TAJIMA and Shinji SATO

Abstract number: 630

Field study

Nearshore sediment process

Tenryu estuary

Image analysis

Shoreline detection

Image rectification

Sand spit erosion

Sand spit collapse